Communication

Zeolite RHO-Type Net with the Lightest Elements

Tao Wu, Jian Zhang, Cong Zhou, Le Wang, Xianhui Bu, and Pingyun Feng

J. Am. Chem. Soc., **2009**, 131 (17), 6111-6113• DOI: 10.1021/ja901725v • Publication Date (Web): 14 April 2009

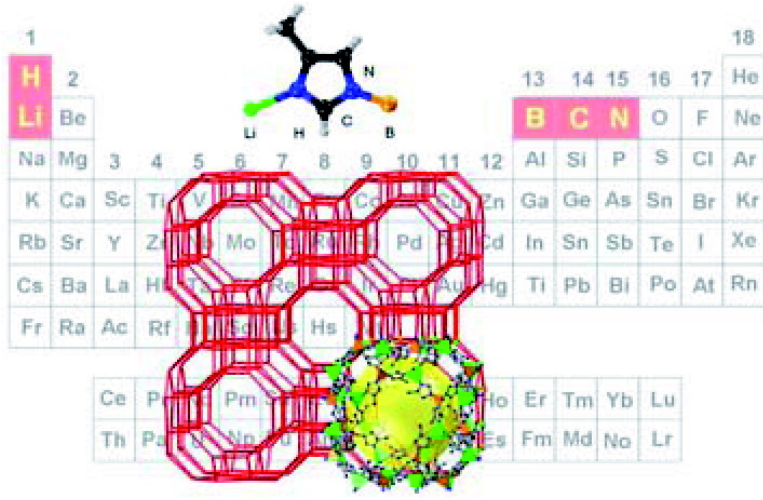

More About This Article

Additional resources and features associated with this article are available within the HTML version:

- Supporting Information
- Access to high resolution figures
- Links to articles and content related to this article
- Copyright permission to reproduce figures and/or text from this article

View the Full Text HTML

J|A|C|S COMMUNICATIONS

Published on Web 04/14/2009

Zeolite RHO-Type Net with the Lightest Elements

Tao Wu, Jian Zhang, Cong Zhou, Le Wang, Xianhui Bu,* and Pingyun Feng*

Department of Chemistry, University of California, Riverside, California 92521, and Department of Chemistry and Biochemistry, California State University, Long Beach, California 90840

Received March 5, 2009; E-mail: pingyun.feng@ucr.edu; xbu@csulb.edu

Crystalline porous materials lie at the center of many industrial applications such as petrochemical refining and air separation.[1,2] The current need for renewable energy and a clean environment further fuels intensive efforts in search of functional porous materials. The early synthetic efforts focused on the replacement of cationic tetrahedral species such as Si^{4+} and Al^{3+} in zeolites with other cations such as P^{5+}, Ge^{4+}, Ga^{3+}, and Co^{2+}.[3−6] The interest in crystalline porous semiconductors has led to the development of porous metal chalcogenides in which the chemistry of anionic species becomes central.[7]

The recent decade has witnessed an explosive growth of metal−organic frameworks (MOFs) which are formed through coordinate bonds between metal cations (or clusters) and organic ligands such as di- or tricarboxlates and diimines.[8−15] A more recent development is the synthesis of covalent organic frameworks (COFs) based on lightweight nonmetallic elements.[16,17] An area that remains largely unexplored is MOCOFs, materials that integrate bonding features (i.e., coordinate and covalent) of both MOFs and COFs. We envisage that the integration between MOFs and COFs should offer a unique opportunity for the development of porous materials that can combine unique advantages of MOFs (e.g., compositional and topological diversity, highly reversible bond formation leading to high crystallinity) and COFs (e.g., lightweight and possibly stronger bond).

We are particularly interested in zeolite-type tetrahedral frameworks, because they offer a wide range of highly porous topological possibilities that can be targeted for the synthetic design. For MOCOFs, we need to consider the selection of nonmetallic as well as metallic elements as the tetrahedral nodes. In this aspect, boron imidazolate anions $(B(im)_4^-$ where *im* is imidazolyl or substituted imidazolyl at 2, 4, and/or 5 positions) represent an ideal tetrahedral building block. When cross-linked with tetrahedral metal cations (e.g., Li^I and Cu^I), neutral zeolite-type frameworks can be expected as illustrated in Scheme 1, in a way analogous to recently reported zinc imidazolates (e.g., ZIFs), a family of MOFs with zeolite-type frameworks [18−24] and a high capacity for CO_2 storage.[23]

Our initial work with boron imidazolate frameworks, however, led to quite dense network topologies such as zni (BIF-1), diamond (BIF-2), and sodalite (BIF-3).[25] Furthermore, the much shorter B−N distance (∼1.5 Å) between boron and the imidazolyl group (as compared to significantly larger metal−ligand distances in MOFs, usually 2.0 Å or larger) tends to narrow the pore aperture and places a serious limitation on the accessibility of internal pore surfaces. As a result, the surface area for a lithium boron 2-methylimidazolate (BIF-3Li) with the sodalite topology is 726 m^2/g, which is only 40% of the surface area for the corresponding zinc 2-methylimidazolate (ZIF-8) with the same topology,[20a,25] negating any potential advantages that the use of such light elements could bring. We reason here that if a more open framework topology could be made,

Scheme 1. Charge Distribution of All Components in Several Neutral Zeolitic Frameworks

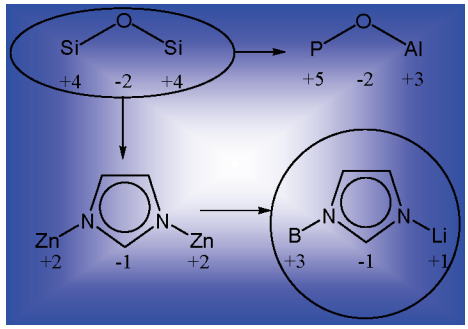

the large window size will more than compensate for the shorter B−N distance and the internal pore volume would then be more accessible.

In the previously reported Zn-*im* system (e.g., ZIFs), the *im*−*im* interaction is known to play a key role in the resultant framework topology.[18−24] The shorter B−N distance in the B-*im* system creates a new challenge because it leads to a closer distance between the adjacent *im* groups, which can dramatically alter interactions between substituent groups on imidazolyl rings. Indeed, while benzimidazole (denoted Bim here) is well-known to form a zeolite RHO type topology (ZIF-11 and ZIF-12),[20a,23a] the reaction of $HB(Bim)_4$ with lithium salts or copper salts only gave layered structures with (4^4) net, with all benzene rings pointed outward away from the 2-D plane (Figure S1). The short B−N distance, coupled with the large benzo group, makes it sterically impossible to form the RHO topology in the boron system. Clearly, the creation of new zeolite-like boron imidazolates requires strategies that take into consideration both synthetic and structural factors unique to boron imidazolates.

In addition, the need for topological control has to be balanced with the need to create maximum porosity. While the size, number, and position of substituent groups on imidazolyl rings do help to generate a more open topology, they can block the pore access. That is why zinc 2-methylimidazolate (ZIF-8) having the relatively dense sodalite net with only 6- and 4-ring windows has a large Langmuir surface area based on N_2 adsorption, whereas zinc benzimidazolate (ZIF-11) having a more open RHO topology with larger 8-, 6-, and 4-rings is actually nonporous toward N_2.[20a] As shown in this work, this anomaly can be prevented by the selection of a suitably substituted imidazolyl ligand that strikes an ideal balance between the structure directing effect and pore window blockage. It is shown here that the boron imidazolate zeolite RHO materials can be created that have a much greater surface area than the boron imidazolate materials with the sodalite net, in distinct contrast with the Zn-*im* system.[20a]

To achieve our goal of creating a more open zeolitic topology with high surface areas (despite the short B−N distance), we choose

Table 1. A Summary of Crystal Data and Refinement Results[a]

code	formula	space group	$a = b = c$ (Å)	net	void space	F.D. (g/cm^3)	aperture diameter (Å)	R (F)
BIF-9-Li	$LiB(4\text{-}Mim)_4$	cubic $P\bar{4}32$	26.2923(3)	3-D, RHO	45.82%	0.750	4.2	0.1161
BIF-9-Cu	$CuB(4\text{-}Mim)_4$	cubic $P\bar{4}32$	26.8152(1)	3-D, RHO	48.24%	0.809	3.3	0.0538

[a] 4-Mim = 4-methylimidazolate. F.D. is framework density.

4-methyl imidazolate (denoted as 4-Mim) as the linker to create the zeolite RHO topology based on the following considerations: (1) 4-position monosubstituted methyl group is smaller than the benzo group in benzimidazole and therefore could better accommodate the shortened B−N distance; and (2) 4- and 5-position *di*-substituted groups are prone to lessen the pore volume of the resulting zeolitic frameworks.

Unlike MOFs in which all tetrahedral nodes can be assembled into a 3-D framework in a one-step synthesis, a two-step procedure, chemical synthesis of $[B(4\text{-}Mim)_4]^-$ and solvothermal assembly between $[B(4\text{-}Mim)_4]^-$ and Li^I/Cu^I, is used to create porous materials here. Crystal structures of pure HB(4-methylimidazolate)$_4$ and its solvated crystal HB(4-methylimidazolate)$_4$·[(±)-2-amino-1-butanol]·H_2O were also determined during this study (Figure S2).

BIF-9-Li and **BIF-9-Cu** with the zeolite RHO topology were synthesized by solvothermal reactions of lithium dicyclohexyl-amide ($LiN[C_6H_{11}]_2$) or copper iodide (CuI) with presynthesized ligand HB(4-methylimidazolate)$_4$, respectively. A large amount of colorless polyhedral single crystals of both **BIF-9-Li** and **BIF-9-Cu** were obtained. Their crystal structures were determined by single crystal X-ray diffraction.

BIF-9-Li crystallizes in a highly symmetrical cubic space group $P\bar{4}32$ (Table 1). The asymmetric unit includes one lithium atom, one boron atom, four 4-methylimidazolate linkers, and half of a disordered solvent benzene molecule. It exhibits a neutral 3-D tetrahedral framework in which each Li^I or B^{III} is tetrahedrally linked to four 4-Mim linkers (B−N bond length 1.486−1.561Å; Li−N bond length 1.961−2.078Å) and each 4-Mim linker bridges one Li^I and one B^{III} with the $Li^I\cdots B^{III}$ distance ranging from 5.263 to 5.554 Å. This distance is much shorter than the $Zn^{II}\cdots Zn^{II}$ distance (∼5.9 Å) in **ZIFs**.[18−23] This 4-connected net with Li and B as tetrahedral nodes has an uninodal zeolite RHO topology (Figure 1). Salient features of the RHO topology include a large α cage with 48 vertices and 4-, 6-, and 8-ring windows. Each α cage is connected to six other α cages by sharing *double 8-ring units* to form a 3-D framework (Figure S3).

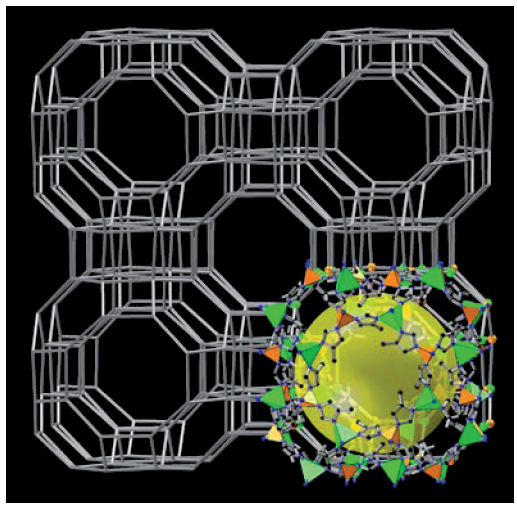

Figure 1. Diagram of RHO topology in $M^IB^{III}(4\text{-}Mim)_4$ ($M^I = Li^+$ or Cu^+). BN_4 tetrahedra are shown in orange, MN_4 tetrahedra in green, N in blue, and C in black. The big yellow sphere represents the void space in the α cage.

Despite the short B−N distance in the B-Mim RHO, both **BIF-9-Li** and **BIF-9-Cu** are porous to N_2 gas while the Zn-Bim RHO (ZIF-11) is not,[20a] because the effect of the small substituent in B-Mim RHO outweights the short B−N distance. As the atom nearest to the center of the cage is hydrogen, the cage diameter (14.4−15.3 Å) and pore aperture diameter (4.2 Å) are calculated by subtracting distances between two diagonal H atoms by twice the *van der Waals* radius of 1.2 Å for the H atom. The cage diameter and the aperture size of the 8-ring is larger than kinetic diameters of most small-molecule gases, which allows **BIF-9-Li** to adsorb various gas molecules that can easily diffuse through the 8-ring aperture (but not through 4- and 6-rings due to their small aperture sizes) (Figure S4). The 8-ring aperture size is also much bigger than that in the corresponding **ZIF** (ZIF-11) with the RHO topology (3.0 Å).[20a] The total potential solvent-accessible volume is 8327.8 Å^3 per unit cell volume, and the pore volume ratio is 45.82% as calculated with the PLATON program.[26]

BIF-9-Cu is isostructural to **BIF-9-Li**. However, the longer bond lengths (B−N bond 1.531−1.551 Å; Cu−N bond 2.006−2.091 Å) in **BIF-9-Cu** leads to a cell parameter (26.8152 Å) slightly larger than that in **BIF-9-Li** (26.2923 Å). Even though **BIF-9-Cu** has a larger solvent-accessible volume (9301.9 Å^3, 48.24%) and unit cell volume (19281.60 Å^3), it has a higher framework density (0.809 g/cm^3) than that of **BIF-9-Li** (0.750 g/cm^3), which results from the large difference in the formular weight.

Thermal gravimetric analysis (TGA) shows both **BIF-9-Li** and **BIF-9-Cu** can be stable up to ∼300 °C under the N_2 atmosphere (Figure S5). The permanent porosity of **BIF-9** was demonstrated by N_2 gas adsorption measurements performed on a Micromeritics ASAP 2010 surface area and pore size analyzer. The samples for surface area analysis were activated by immersing as-synthesized **BIF-9** with suitable solvents (see Supporting Information), followed by evacuation at room temperature. The activated samples were characterized by XRD to confirm the structural integrity (Figure S7 and S8). **BIF-9** exhibits type I adsorption isotherm behavior

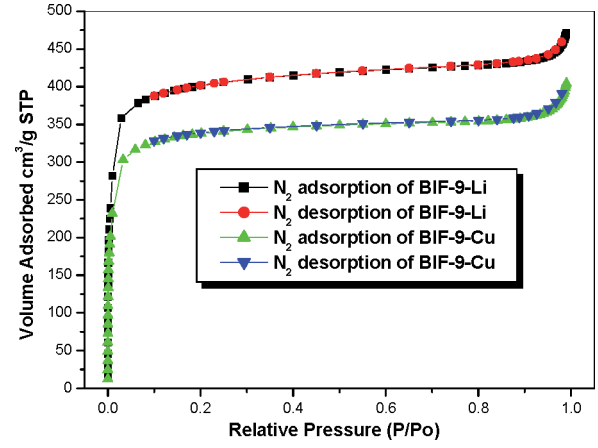

Figure 2. Nitrogen gas sorption isotherm at 77 K for **BIF-9-Li** and **BIF-9-Cu**. P/P_0 is the ratio of gas pressure (P) to saturation pressure (P_0), with P_0 = 770 Torr.

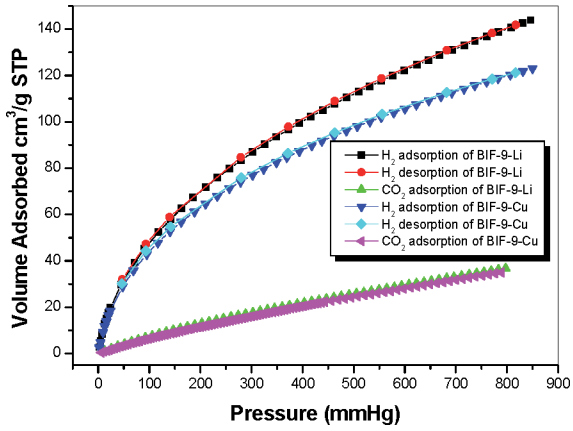

Figure 3. Gas sorption isotherm of **BIF-9-Li** and **BIF-9-Cu** for H_2 at 77 K and for CO_2 at 273 K.

typical of materials with permanent microporosity (Figure 2). The Langmuir surface areas were 1818 and 1524 m^2/g for **BIF-9-Li** and **BIF-9-Cu**, respectively, demonstrating the effect of molecular weight. The BET method yields surface areas of 1523 and 1287m^2/g, respectively. A single data point at relative pressure 0.500 gives a maximum micropore volume of 0.648 and 0.540 cm^3/g, respectively, by the Horvath−Kawazoe equation.

Hydrogen adsorption studies revealed that **BIF-9-Li** can adsorb 1.23 wt% (volumetric uptake of 9.23 kg/m^3, calculated density: 0.750 g/cm^3) hydrogen at 760 Torr and 77 K, significantly higher than that of **BIF-9-Cu** (1.06 wt %; volumetric uptake of 8.58 kg/m^3, calculated density: 0.809 g/cm^3) (Figure 3). CO_2 adsorption isotherms of **BIF-9** were also investigated. The amounts being adsorbed at 760 Torr and 273 K reach 35.6 cm^3/g (1.60 mmol/g) and 34.1 cm^3/g (1.53 mmol/g) for **BIF-9-Li** and **BIF-9-Cu**, respectively. The lighter framework density of **BIF-9-Li** may be an important contributing factor for the better gas uptake behavior of **BIF-9-Li** vs **BIF-9-Cu**.

In conlusion, reported here are two highly porous examples of MOCOFs, a new family of framework materials seamlessly integrating the coordinate bonds of metal−organic frameworks (MOFs) and covalent bonds of covalent organic framework materials (COFs). These two materials represent the lightest zeolite RHOs known to date. Their synthesis is an extraordinary example in which the structure-directing effect of the substituent groups on the cross-linking imidazolyl ring strikes an ideal balance with their pore narrowing effect, leading to the creation of a very open zeolite RHO topology with highly accessible internal pores.

Acknowledgment. We thank the support of this work by the NSF (P.F., CHEM-0809335; X. B., DMR-0846958). P.F. is a Camille Dreyfus Teacher Scholar, and X.B. is a Henry Dreyfus Teacher Scholar.

Supporting Information Available: Five additional figures; experimental procedures for the preparation of boron imidazle ligands and its coordination polymers; detailed TGA plots; as-synthesized and simulated X-ray powder diffraction patterns; crystallographic data including positional parameters, thermal parameters, and bond distances and angles (.CIF). These materials are available free of charge via the Internet at http://pubs.acs.org.

References

(1) Davis, M. E. *Nature (London)* **2002**, *417*, 813–821.
(2) Van Bekkum, H.; Flanigen, E. M.; Jacobs, P. A; Jansen, J. C. *Introduction to Zeolite Science and Practice*; Elsevier: Amsterdam, 2001.
(3) Wilson, S. T.; Lok, B. M.; Messina, C. A.; Cannan, T. R.; Flanigen, E. M. *J. Am. Chem. Soc.* **1982**, *104*, 1146–1147.
(4) Cheetham, A. K.; Férey, G.; Loiseau, T. *Angew. Chem., Int. Ed.* **1999**, *38*, 3268–3292.
(5) (a) Cooper, E. R.; Andrews, C. D.; Wheatley, P. S.; Webb, P. B.; Wormald, P.; Morris, R. E. *Nature (London)* **2004**, *430*, 1012–1016. (b) Parnham, E. R.; Morris, R. E. *J. Am. Chem. Soc.* **2006**, *128*, 2204–2205. (c) Parnham, E. R.; Morris, R. E. *Acc. Chem. Res.* **2007**, *40*, 1005–1013.
(6) (a) Bu, X.; Feng, P.; Stucky, G. D. *Science* **1997**, *278*, 2080–2085. (b) Feng, P.; Bu, X.; Stucky, G. D. *Nature (London)* **1997**, *388*, 735–740.
(7) (a) Bedard, R. L.; Wilson, S. T.; Vail, L. D.; Bennett, J. M.; Flanigen, E. M. In *Zeolites: Facts, Figures, Future. Proceedings of the 8th International Zeolite Conference*; Jacobs, P. A., van Santen, R. A., Eds.; Elsevier: Amsterdam, 1989; p 375. (b) Zheng, N.; Bu, X.; Wang, B.; Feng, P. *Science* **2002**, *298*, 2366–2369. (c) Li, H. L.; Laine, A.; O'Keeffe, M.; Yaghi, O. M. *Science* **1999**, *283*, 1145–1147.
(8) (a) Mulfort, K. L.; Farha, O. K.; Stern, C. L.; Sarjeant, A. A.; Hupp, J. T. *J. Am. Chem. Soc.* **2009**, *131*, 3866–3868. (b) Mulfort, K. L.; Hupp, J. T. *J. Am. Chem. Soc.* **2007**, *129*, 9604–9605.
(9) Yaghi, O. M.; O'Keeffe, M.; Ockwig, N. W.; Chae, H. K.; Eddaoudi, M.; Kim, J. *Nature (London)* **2003**, *423*, 705–714.
(10) Morris, R. E.; Wheatley, P. S. *Angew. Chem., Int. Ed.* **2008**, *47*, 2–20.
(11) (a) Férey, G. *Chem. Soc. Rev.* **2008**, *37*, 191–214. (b) Férey, G.; Serre, C.; Millange, F.; Surble, S.; Dutour, J.; Margiolaki, I. *Angew. Chem., Int. Ed.* **2004**, *43*, 6296–6301.
(12) (a) Evans, O. R.; Lin, W. *Acc. Chem. Res.* **2002**, *35*, 511–512. (b) Kesanli, B.; Lin, W. *Coord. Chem. Rev.* **2003**, *246*, 305–326.
(13) Moulton, B.; Zaworotko, M. J. *Chem. Rev.* **2001**, *101*, 1629–1658.
(14) Zhao, D.; Yuan, D.; Zhou, H.-C. *Energy Environ. Sci.* **2008**, *1*, 222–235.
(15) Kitagawa, S.; Kitaura, R.; Noro, S. *Angew. Chem., Int. Ed.* **2004**, *43*, 2334–2375.
(16) (a) Côté, A. P.; Benin, A. I.; Ockwig, N.W.; O'Keeffe, M.; Matzger, A. J.; Yaghi, O. M. *Science* **2005**, *310*, 1166–1170. (b) El-Kaderi, H. M.; Hunt, J. R.; Mendoza-Cortés, J. L.; Côté, A. P.; Taylor, R. E.; O'Keeffe, M.; Yaghi, O. M. *Science* **2007**, *16*, 268–272. (c) Côté, A. P.; El-Kaderi, H. M.; Furukawa, H.; Hunt, J. R.; Yaghi, O. M. *J. Am. Chem. Soc.* **2007**, *129*, 12914–12915.
(17) (a) Wan, S.; Guo, J.; Kim, J.; Ihee, H.; Jiang, D. *Angew. Chem., Int. Ed.* **2008**, *47*, 8826–8830. (b) Kuhn, P.; Antonietti, M.; Thomas, A. *Angew. Chem., Int. Ed.* **2008**, *47*, 3450–3453. (c) Tilford, R. W.; Mugavero, S. J., III; Pellechia, P. J.; Lavigne, J. J. *Adv. Mater.* **2008**, *20*, 2741–2746.
(18) (a) Tian, Y. Q.; Cai, C. X.; Ji, Y.; You, X. Z.; Peng, S. M.; Lee, G. S. *Angew. Chem., Int. Ed.* **2002**, *41*, 1384–1386. (b) Tian, Y. Q.; Cai, C. X.; Ren, X. M.; Duan, C. Y.; Xu, Y.; Gao, S.; You, X. Z. *Chem.—Eur. J.* **2003**, *9*, 5673–5685. (c) Tian, Y.-Q.; Chen, Z. X.; Weng, L.-H.; Guo, H. B.; Gao, S.; Zhao, D. Y. *Inorg. Chem.* **2004**, *43*, 4631–4635. (d) Tian, Y.-Q.; Zhao, Y.-M.; Chen, Z.-X.; Zhang, G.-N.; Weng, L.-H.; Zhao, D.-Y. *Chem.—Eur. J.* **2007**, *13*, 4146–4154.
(19) Huang, X.-C.; Lin, Y.-Y.; Zhang, J. P.; Chen, X.-M. *Angew. Chem., Int. Ed.* **2006**, *45*, 1557–1559.
(20) (a) Park, K. S.; Ni, Z.; Côté, A. P.; Choi, J. Y.; Huang, R.; Uribe-Romo, F. J.; Chae, H. K.; O'Keeffe, M.; Yaghi, O. M. *Proc. Natl. Acad. Sci. U.S.A.* **2006**, *103*, 10186–10191. (b) Hayashi, H.; Côté, A. P.; Furukawa, H.; O'Keeffe, M.; Yaghi, O. M. *Nat. Mater.* **2007**, *6*, 501–506.
(21) (a) Morris, W.; Doonan, C. J.; Furukawa, H.; Banerjee, R.; Yaghi, O. M. *J. Am. Chem. Soc.* **2008**, *130*, 12626–12627. (b) Banerjee, R.; Furukawa, H.; Britt, D.; Knobler, C.; O'Keeffe, M.; Yaghi, O. M. *J. Am. Chem. Soc.* **2009**, *131*, 3875–3877.
(22) (a) Wu, T.; Bu, X.; Zhang, J.; Feng, P. *Chem. Mater.* **2008**, *20*, 7377–7382. (b) Wu, T.; Bu, X.; Liu, R.; Lin, Z.; Zhang, J.; Feng, P. *Chem.—Eur. J.* **2008**, *14*, 7771–7773.
(23) (a) Banerjee, R.; Phan, A.; Wang, B.; Knobler, C.; Furukawa, H.; O'Keeffe, M.; Yaghi, O. M. *Science* **2008**, *319*, 939–943. (b) Wang, B.; Côté, A. P.; Furukawa, H.; O'Keeffe, M.; Yaghi, O. M. *Nature (London)* **2008**, *453*, 207–211.
(24) (a) Liu, Y. L.; Kravtsov, V.; Larsen, R.; Eddaoudi, M. *Chem. Commun.* **2006**, 1488–1490. (b) Sava, D. F.; Kravtsov, V.; Nouar, F.; Wojtas, L.; Eubank, J. F.; Eddaoudi, M. *J. Am. Chem. Soc.* **2008**, *130*, 3768–3770. (c) Nouar, F.; Eckert, J.; Eubank, J. F.; Forster, P.; Eddaoudi, M. *J. Am. Chem. Soc.* **2009**, *131*, 2864–2870.
(25) Zhang, J.; Wu, T.; Zhou, C.; Chen, S.; Feng, P.; Bu, X. *Angew. Chem., Int. Ed.* **2009**, *48*, 2542–2545.
(26) Spek, A. L. *J. Appl. Crystallogr.* **2003**, *36*, 7–13.

JA901725V